OXFORD

Human Molecular Genetics, 2017, Vol. 26, No. 12 2299–2306

doi: 10.1093/hmg/ddx121
Advance Access Publication Date: 3 April 2017
Original Article

ORIGINAL ARTICLE

Two pathways of rod photoreceptor cell death induced by elevated cGMP

Tian Wang[1], Stephen H. Tsang[2,3] and Jeannie Chen[1,*]

[1]Zilkha Neurogenetic Institute, Department of Cell & Neurobiology, Keck School of Medicine, University of Southern California, Los Angeles, CA 90089, USA, [2]Jonas Children's Vision Care, and Bernard & Shirlee Brown Glaucoma Laboratory, Departments of Ophthalmology and Pathology & Cell Biology, Institute of Human Nutrition, Herbert Irving Comprehensive Cancer Center, Columbia University, NY 10032, USA and [3]Edward S. Harkness Eye Institute, New York-Presbyterian Hospital, NY 10032, USA

*To whom correspondence should be addressed at: Zilkha Neurogenetic Institute, 1501 San Pablo Street, room 227, Los Angeles, CA 90089, USA. Email: jeannie@usc.edu

Abstract

Cyclic-GMP is a second messenger in phototransduction, a G-protein signaling cascade that conveys photon absorption by rhodopsin to a change in current at the rod photoreceptor outer segment plasma membrane. Basal cGMP level is strictly controlled by the opposing actions of phosphodiesterase (PDE6) and retinal guanylyl cyclases (GCs), and mutations in genes that disrupt cGMP homeostasis leads to retinal degeneration in humans through mechanisms that are incompletely understood. The purpose of this study is to examine two distinct cellular targets of cGMP: the cGMP-gated (CNG) channels and protein kinase G (PRKG), and how each may contribute to rod cell death. Using a mouse genetic approach, we found that abolishing expression of CNG channels prolongs rod survival caused by elevated cGMP in a PDE6 mutant mouse model. This observation supports the use of channel blockers to delay rod death, which is expected to prolong useful vision through enhanced cone survival. However, the absence of CNG channel alone also caused abnormal cGMP accumulation. In a mouse model of CNG channel loss-of-function, abolishing PRKG1 expression had a long-lasting effect in promoting rod cell survival. Our data strongly implicate two distinct cGMP-mediated cell death pathways, and suggest that therapeutic designs targeting both pathways will be more effective at slowing photoreceptor cell death caused by elevated cGMP.

Introduction

Many forms of human blindness have their etiology in genetic mutations associated with increased cGMP levels. For example, mutations in guanylyl cyclase activating proteins (GCAPs), PDE6 and the cyclic-nucleotide-gated (CNG) channels have been linked to autosomal dominant cone dystrophy, cone rod dystrophy, retinitis pigmentosa, achromatopsia and macular degeneration in humans (1–10). However, the mechanism by which elevated cGMP levels lead to photoreceptor death is still unclear. Cyclic GMP is the second messenger that conveys photon absorption by rod or cone opsins to a change in current at the plasma membrane (11). In darkness, cGMP concentration is controlled by the dynamic equilibrium of its synthesis and hydrolysis by the basal activities of retinal membrane guanylyl cyclases (GCs) and phosphodiesterase (PDE6), respectively (Fig. 1A). The free cGMP in darkness maintains ~3% of the cyclic nucleotide-gated ion (CNG) channels in the open state to form the circulating dark current by the influx of Na^+ and Ca^{2+} into the outer segment and extrusion of Na^+ by the Na^+/K^+ pump at the inner segment (12,13). In rods, photon absorption by rhodopsin leads to a conformational change in this prototypical G-protein coupled receptor, allowing it to bind and activate transducin. Transducin then binds the inhibitory γ-subunit of PDE6, releasing the catalytic PDE6αβ subunits to hydrolyze cGMP.

Received: December 19, 2016. **Revised:** February 24, 2017. **Accepted:** March 22, 2017

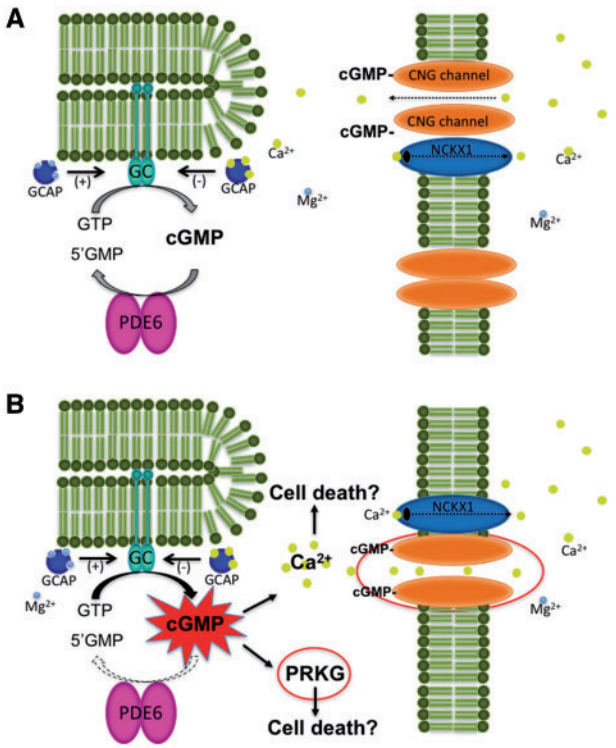

Figure 1. Phototransduction proteins involved in cGMP m2etabolism in health and disease. (**A**) In darkness, [cGMP] is determined by the basal activities of phosphodiesterase (PDE6) and retinal guanylyl cyclases (GC). PDE6 activity is stimulated when light-activated transducin removes the inhibitory PDE6γ subunit from the catalytic PDE6αβ subunits. Degradation of cGMP causes the cGMP-gated channels to close, preventing Na^+ and Ca^{2+} influx and lowering $[Ca^{2+}]$ due to its continued extrusion by NCKX1. GC activity is Ca^{2+}-sensitive through its interaction with Ca^{2+}-binding proteins, guanylyl cyclase activating proteins 1 and 2 (GCAP). In darkness, Ca^{2+} enters the cell through open cGMP-gated channels. Under high $[Ca^{2+}]$, Ca^{2+}-bound GCAP inhibits basal GC activity. When $[Ca^{2+}]$ in the outer segment falls following light exposure, GCAP becomes Mg^{2+}-bound and stimulates GC to synthesize cGMP. (**B**) Dominant mutations in GCAPs that activate GC or loss-of-function mutations in PDE6 lead to elevated [cGMP], which in turn can cause excessive Ca^{2+} influx through the open CNG channels or stimulation of PRKG activity, leading to cell death.

The subsequent decline of cGMP concentrations leads to the closure of CNG channels and the reduction of the dark current as well as lowering of intracellular $[Ca^{2+}]$, due to its reduced influx and continuous extrusion by the Na^+/Ca^{2+}-K^+ exchanger, NCKX1 (14,15). Low intracellular $[Ca^{2+}]$ activates guanylyl cyclase activating proteins (GCAPs) to stimulate GCs to increase cGMP synthesis (16–18), and rising [cGMP] opens CNG channels and facilitates the recovery of the light response (19,20). In this manner the opposing actions of PDE6 and GCs set the cGMP concentration (Fig. 1 A), and mutations that lead to PDE6 loss-of-function or GC gain-of-function can lead to cGMP accumulation followed by cell death (Fig. 1B).

One potential cellular target of cGMP toxicity is the CNG channel (Fig. 1B). Given that the cooperativity of CNG channel activation by cGMP is 3 (21–23), a small increase in [cGMP] will produce an 8-fold change in the relative Ca^{2+} influx. Therefore, uncontrolled Ca^{2+} influx through an excessive number of open CNG channels has been suggested as a mechanism for cGMP-induced photoreceptor cell death (8). In support of this mechanism, reducing CNG channel expression slows the retinal degeneration in mouse models that harbor loss-of-function *Pde6* mutations (24–26). Whether this mechanism applies broadly to photoreceptor cell death associated with increased cGMP is not known.

Another cellular target for cGMP is cGMP-dependent protein kinase G (PRKG, Fig. 1B). Its increased activity was observed in the *rd1* and *rd2* mouse models that harbor loss-of-function mutations in *Pde6b* and *Prph2* genes, respectively (27). It should be noted that cGMP accumulation is a hallmark of *rd1* (28,29), but not *rd2* retina. Nevertheless, application of small molecule inhibitors of PRKG demonstrated a modest effect in slowing retinal degeneration in both mouse models (27). Although this pharmacologic approach provides supporting evidence for photoreceptor cell death mediated by PRKG, small molecule inhibitors may have additional unintended cellular targets, and direct demonstration of a causal relationship between PRKG activation and retinal degeneration is still lacking.

Massive accumulation of cGMP in rods and cones also occurs when the respective CNG channels are absent (10,30–32). This increase in cGMP is likely a primary cause of cell death, since a rescuing effect is observed when expression of guanylyl cyclase is lowered (10,25,26). In addition, the activity and expression levels of PRKG appeared increased in *Cnga3*$^{-/-}$ mice deficient in the cone CNG channel, correlating PRKG activation with cone cell death (10). As in rods, a causal link between PRKG activity and cone death remains to be established.

In this study, we utilized mouse genetics to examine the involvement of CNG channels and PRKG in two different mouse models of cGMP-induced retinal degeneration. The first is the *Pde6g*$^{-/-}$ mice that exhibit reduced PDE6 activity and cGMP accumulation (33); the second is *Cngb1*$^{-/-}$ mice that are deficient in rod CNG channel function (15,34) (see also (35,36)). *Pde6g*$^{-/-}$ mice were crossed into the *Cngb1*$^{-/-}$ or *Prkg1*$^{-/-}$ (lacking Prkg1) (37) background to investigate the involvement of each target for mediating cGMP-induced cell death. Retinae from *Prkg1*$^{-/-}$ mice do not degenerate, and the slow rate of retinal degeneration in *Cngb1*$^{-/-}$ mice relative to *Pde6g*$^{-/-}$ (~4 months vs. 3 weeks) allowed us to separate the effects of each mutation. We also generated *Prkg1*$^{-/-}$*Cngb1*$^{-/-}$ double knockout mice to determine whether PRKG1 activation is involved in *Cngb1*$^{-/-}$ rod cell death.

Results

Retinal degeneration in *Pde6g*$^{-/-}$ mice is delayed in the *Cngb1* null background

Mice lacking the inhibitory PDE6γ subunit exhibit rapid retinal degeneration due to loss of structure and function of the PDE6 holoenzyme, which in turn leads to cGMP accumulation (33). If the CNG channel is the primary target of elevated [cGMP] in this retinal degeneration model, then down-regulating channel expression should delay rod death. We crossed *Pde6g*$^{-/-}$ mice with *Cngb1*$^{-/-}$ mice and compared retinal morphology from age-matched *Cngb1*$^{-/-}$, *Pde6g*$^{-/-}$ single knockout mice and *Pde6g*$^{-/-}$*Cngb1*$^{-/-}$ double knockout mice to test this hypothesis (Fig. 2A). The thickness of the outer nuclear layer (Fig. 2A, ONL) of the mouse retina reflects the approximate number of rods because they consist of 95–97% of the photoreceptor cell population (38). At age 2 weeks (Fig. 2A, left panels), the *Cngb1*$^{-/-}$ retinae resembled that of control C57 mice (not shown) whereas the ONL of *Pde6g*$^{-/-}$ retinae was reduced by ~80%. This large-scale rod loss was averted in *Pde6g*$^{-/-}$*Cngb1*$^{-/-}$ retinae. At 3 weeks of age (Fig. 2A, middle panels), the ONL thickness of *Cngb1*$^{-/-}$ retina was slightly reduced. However, only one cell layer consisting of cones remained in the ONL of *Pde6g*$^{-/-}$ mice. In contrast, the *Pde6g*$^{-/-}$*Cngb1*$^{-/-}$ retina was much better preserved, with 4–5

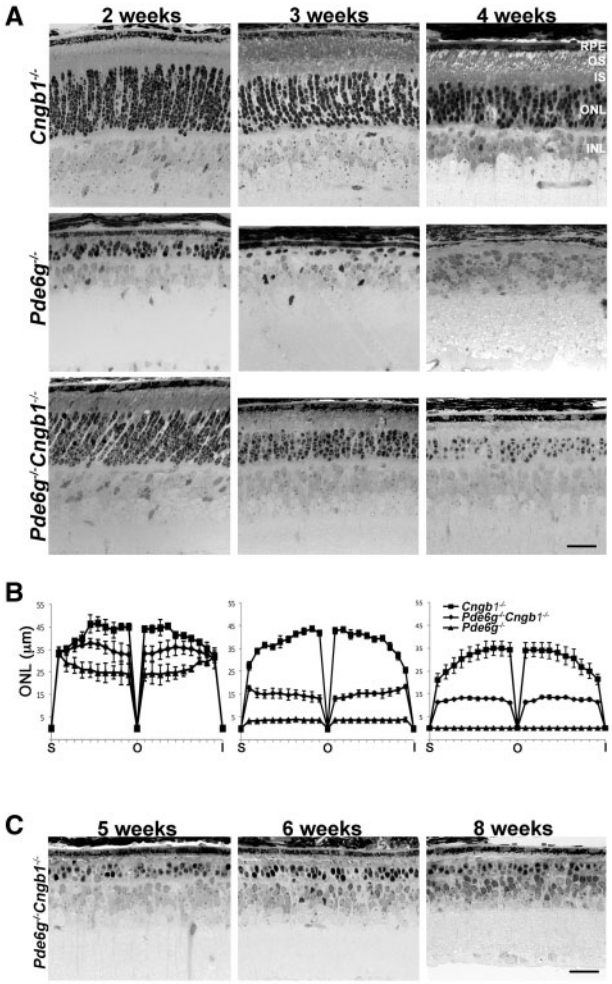

Figure 2. Retinal degeneration of *Pde6g*$^{-/-}$ mice is delayed in the *Cngb1*$^{-/-}$ background. (**A**) Retinal morphology of age-matched *Cngb1*$^{-/-}$, *Pde6g*$^{-/-}$ and *Pde6g*$^{-/-}$*Cngb1*$^{-/-}$ mice at age 2, 3 and 4 weeks. Rod death is much more rapid in the *Pde6g*$^{-/-}$ retina when compared to that of *Cngb1*$^{-/-}$ mice, and abolishing CNG channel expression in *Pde6g*$^{-/-}$ retinae substantially slowed rod death. RPE, retinal pigmented epithelium; OS: outer segment; IS, inner segment; ONL, outer nuclear layer; INL, inner nuclear layer. (**B**) Quantification of ONL thickness (mean ± SD, $N \geq 3$) across the entire span of the central retina from the indicated mice at 2, 3 and 4 weeks of age. Squares: *Cngb1*$^{-/-}$; diamonds: *Pde6g*$^{-/-}$*Cngb1*$^{-/-}$; triangles, *Pde6g*$^{-/-}$. S: superior; I, inferior; O, optic nerve. (**C**). Retinal morphology of *Pde6g*$^{-/-}$ *Cngb1*$^{-/-}$ mice at age 5, 6 and 8 weeks. Scale bars = 20 μm.

layers of nuclei remaining in the ONL. At 4 weeks (Fig. 2A, right panels), the *Cngb1*$^{-/-}$ retina showed a 20% reduction in the ONL layer. All photoreceptor cell nuclei have disappeared in the *Pde6g*$^{-/-}$ retina, and a thinning of the adjacent retinal pigmented epithelium (RPE) was also observed. Interestingly, the rescuing effect of *Cngb1*$^{-/-}$ in the *Pde6g*$^{-/-}$ retina was still apparent at this age. Morphometric measurements of the ONL thickness (mean ± SD) across the entire span of the retina from these mice at the indicated ages are shown in Figure 2B. The effect of the rescue of *Pde6g*$^{-/-}$ by *Cngb1*$^{-/-}$ lasts beyond 8 weeks, although cell death was not fully halted (Fig. 2C). These results are consistent with previous reports (24,25) utilizing other PDE6 mutants that implicate the CNG channel as a target of cGMP-induced toxicity. However, that CNG channel deficiency delayed, but did not halt *Pde6g*$^{-/-}$ rod death, suggests additional cGMP-mediated cell death pathways exist.

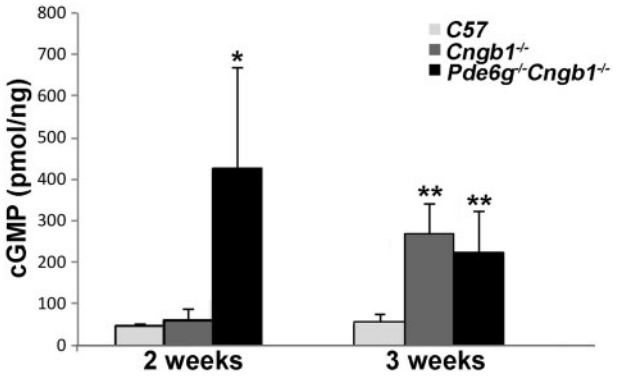

Figure 3. cGMP is elevated in the *Cngb1*$^{-/-}$ and *Pde6g*$^{-/-}$*Cngb1*$^{-/-}$ retinae. Cyclic GMP levels were measured using enzyme-linked immunosorbent assay (ELISA) in retinal extract prepared from the indicated mice at 2 weeks ($N \geq 4$ for each group) or 3 weeks of age ($N \geq 4$ for each group). Differences within groups were first interrogated by one way ANOVA, and pair-wise comparisons were made by 2-tailed *t*-test. $^{**}P < 0.01$, $^{*}P = 0.0006$.

cGMP is elevated in the *Cngb1*$^{-/-}$ and *Pde6g*$^{-/-}$*Cngb1*$^{-/-}$ retinae

We next quantified cGMP concentrations in retinal extracts from control C57, *Cngb1*$^{-/-}$, and *Pde6g*$^{-/-}$*Cngb1*$^{-/-}$ retinae to see how their cGMP levels correlate with retinal degeneration. Because light exposure leads to cGMP degradation by PDE6, mice were dark-adapted overnight and all experimental preparations were performed under infrared light to measure basal levels of cGMP (Fig. 3). One-way analysis of variance (ANOVA) showed that the cGMP levels in retinae from C57, *Cngb1*$^{-/-}$ and *Pde6g*$^{-/-}$*Cngb1*$^{-/-}$ mice were significantly different at 2 weeks of age ($P = 0.0006$, Fig. 3). Post-hoc Tukey HSD test showed no difference between retinae from C57 and *Cngb1*$^{-/-}$ mice ($P = 0.9$), but a significant difference between these values and that of *Pde6g*$^{-/-}$*Cngb1*$^{-/-}$ retinae ($P = 0.004$ and $P = 0.001$, respectively). The elevated cGMP in *Pde6g*$^{-/-}$*Cngb1*$^{-/-}$ retinae relative to that of *Cngb1*$^{-/-}$ samples is likely due to PDE6 loss-of-function. One-way ANOVA was again applied to cGMP levels measured from 3-week old mice, wherein a significant difference was detected between the three groups ($P = 0.0058$). Post-hoc Tukey HSD showed that both the cGMP levels of *Cngb1*$^{-/-}$ and *Pde6g*$^{-/-}$*Cngb1*$^{-/-}$ samples were significantly higher than that of C57 ($P = 0.006$ and $P = 0.02$, respectively), but the values between *Cngb1*$^{-/-}$ and *Pde6g*$^{-/-}$*Cngb1*$^{-/-}$ samples were not different ($P = 0.65$). The ~5-fold increase in cGMP levels in *Cngb1*$^{-/-}$ retinae is consistent with previous reports (30,32). The mechanism for this increase is not known, but may be related to a persistently low intracellular [Ca^{2+}] due to a lack of entry through CNG channels and its continued extrusion through NCKX1, leading to GC activation by GCAPs (Fig. 1). Although the cGMP level was still elevated in the *Pde6g*$^{-/-}$*Cngb1*$^{-/-}$ retinae at 3 weeks relative to control C57 mice, it is lower than the values in 2-week-old *Pde6g*$^{-/-}$*Cngb1*$^{-/-}$ mice, a result consistent with ongoing rod cell death (Fig. 2). Together, these data implicate other cellular target(s), aside from the CNG channel, for cell death induced by elevated [cGMP].

Prkg1 knockout does not rescue the degeneration of *Pde6g*$^{-/-}$ retinae

The role of PRKG as a target of cGMP-mediated toxicity in PDE6 loss-of-function mutations was suggested by previous evidence

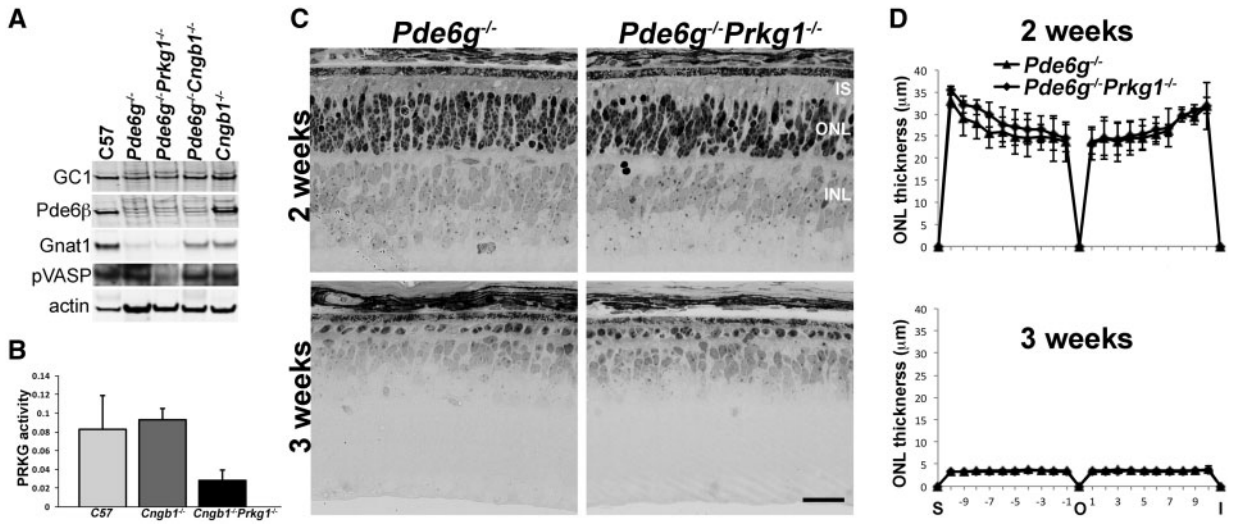

Figure 4. PRKG1 deficiency does not delay retinal degeneration in *Pde6g*$^{-/-}$ mice. (**A**) Immunoblots of retinal homogenates from age-matched (2 weeks old) mice of the indicated genotypes. Rod transducin-α (GNAT1) was used as an indicator of rod loss. Actin served as a loading control. (**B**) Cyclic-GMP stimulated PRKG activity in retinal extracts from the indicated mice ($N \geq 3$). One-way ANOVA revealed a significant difference in the group of values ($P = 0.0004$). Post-hoc Tukey HSD test showed no difference between C57 and *Cngb1*$^{-/-}$ samples, whereas the value of *Cngb1*$^{-/-}$*Prkg1*$^{-/-}$sample was significantly different from both C57 and *Cngb1*$^{-/-}$ samples ($P < 0.01$). (**C**) Retinal morphology of *Pde6g*$^{-/-}$ and *Pde6g*$^{-/-}$*Prkg1*$^{-/-}$ littermates at age 2 weeks and 3 weeks. IS: inner segment; ONL: outer nuclear layer; INL, inner nuclear layer. Scale bar = 20 μm. (**D**) Measurements of outer nuclear layer thickness across the span of the retina at the central meridian (mean ± SD, $N \geq 3$). Triangles: *Pde6g*$^{-/-}$; diamonds: *Pde6g*$^{-/-}$*Prkg1*$^{-/-}$. S, superior; I, inferior; O, optic nerve.

of PRKG activation and efficacy of PRKG inhibitors in slowing retinal degeneration in *rd1* mice (27). Mice and humans express three different isoforms of PRKG: *Prkg1α* and *Prkg1β*, splice variants from the same *Prkg1* gene, and *Prkg2* (39). *Prkg1* expression is highest in the eye relative to other tissues (lung, intestine and brain), whereas *Prkg2* expression was lowest in the eye and highest in the intestines (40). We, therefore, sought to examine the potential role of *Prkg1* activation in cGMP-induced rod death. Although *Prkg1*$^{-/-}$ mice survive to adulthood (37), they do not breed well. Therefore, *Pde6g*$^{-/-}$*Prkg1*$^{+/-}$ mice were crossed to generate *Pde6g*$^{-/-}$*Prkg1*$^{-/-}$ double knockout mice as well as control *Pde6g*$^{-/-}$*Prkg1*$^{+/+}$ littermates. First, western blots were performed on retinal homogenates prepared from 2 week-old mice of the indicated genotypes (Fig. 4A). Consistent with the earlier report (33), the absence of the inhibitory PDE6γ subunit led to structural instability of the holoenzyme and hence lower levels of the PDE6 catalytic subunits. The level of GC1 was also reduced, albeit to a lesser extent. This reduction in GC1, as well as that of the α-subunit of rod transducin (Gnat1), likely reflects rod loss (Figs 2A and 4C). The relative retention of GC enzyme levels compared to that of PDE6 provides a plausible explanation for the pathologic accumulation of cGMP in these mice (Fig. 3). To detect PRKG activity, we utilized an antibody against phosphor-VASP (Ser239), which monitors PRKG activation and signaling (41). As shown in Figure 4A, phosphor-VASP signal was present in control C57, *Pde6g*$^{-/-}$, *Cngb1*$^{-/-}$and *Pde6g*$^{-/-}$*Cngb1*$^{-/-}$ retinal homogenates at 2 weeks, but was largely absent in the age-matched *Pde6g*$^{-/-}$*Prkg1*$^{-/-}$ double knockout retinae. As an independent test, the level of PRKG enzyme, as revealed by cGMP-stimulated PRKG activity *in vitro*, was also directly measured from the retinal homogenates of *C57*, *Cngb1*$^{-/-}$ and *Cngb1*$^{-/-}$*Prkg1*$^{-/-}$ double knockout mice (Fig. 4B). No difference was observed between C57 and *Cngb1*$^{-/-}$ samples, whereas the value was significantly lower for *Cngb1*$^{-/-}$*Prkg1*$^{-/-}$ double knockout samples ($P < 0.01$). We then compared retinal morphology of *Pde6g*$^{-/-}$ and *Pde6g*$^{-/-}$*Prkg1*$^{-/-}$ littermates at 2 and 3 weeks of age. No difference in the retinal morphology or degree of degeneration was observed between mice of these different genotypes (Fig. 4C). This lack of effect is also evident in the western blots that showed similar low levels of rod transducin-alpha (Gnat1) and GC1 in the retinal homogenates of *Pde6g*$^{-/-}$ and *Pde6g*$^{-/-}$*Prkg1*$^{-/-}$ mice when compared to the *Pde6g*$^{-/-}$*Cngb1*$^{-/-}$ sample, reflecting rod rescue by *Cngb1*$^{-/-}$ but not *Prkg1*$^{-/-}$ (Fig. 4A). Measurements of ONL thickness at 2 weeks (Fig. 4D, upper panel) and 3 weeks (Fig. 4D, lower panel) showed no difference between *Pde6g*$^{-/-}$ and *Pde6g*$^{-/-}$*Prkg1*$^{-/-}$ mice. Together, these data show that the CNG channel, but not PRKG1, is a primary cellular target for cGMP-induced cellular toxicity for *Pde6* loss-of-function mutations. These results suggest that cGMP accumulation caused by other genetic mutations also acts through the CNG channel when the channel is present and functional.

Prkg1 knockout slows degeneration of *Cngb1*$^{-/-}$ retinae

As shown in Figure 3, the cGMP levels were abnormally high in *Cngb1*$^{-/-}$ retinae by 3 weeks of age when compared to C57 retinae. To investigate the involvement of PRKG in the retinal degeneration of *Cngb1*$^{-/-}$ mice, *Cngb1*$^{-/-}$ *Prkg1*$^{+/-}$ mice were mated to generate littermate *Cngb1*$^{-/-}$ and *Cngb1*$^{-/-}$*Prkg1*$^{-/-}$ mice, and their retinal morphology at 3 months of age was compared (Fig. 5). Retinal degeneration of *Cngb1*$^{-/-}$mice at this age exhibits a graded pattern, with the central-inferior region showing a higher number of surviving rods (Fig. 5A). In these regions, the ONL of *Cngb1*$^{-/-}$*Prkg1*$^{-/-}$ retinae appeared thicker than that of *Cngb1*$^{-/-}$ littermates. Measurement of ONL thickness of these mice is presented in Figure 5B (mean ± SD), where a statistical significance was detected at the central-inferior regions (Fig. 5B, asterisks represent $P < 0.05$, 2-tailed *t*-test). This rescuing effect extends to 4- (Fig. 6A) and 5-month old (Fig. 6B) mice. At these ages, retinae from *Cngb1*$^{-/-}$ show a single row of ONL, whereas retinae from the *Cngb1*$^{-/-}$*Prkg1*$^{-/-}$ littermates contained 3 to 4 rows of ONL (Fig. 6A and B). To see whether cones were retained in these retinae, retinal sections were stained for peanut

agglutinin (PNA), a cone marker. Consistent with the region of greater ONL thickness, PNA reactivity can be seen in the central-inferior pole of the retina (Fig. 6C). Together, these results suggest that PRKG1 activity plays a role in cell death associated with elevated cGMP caused by the absence of the CNG channel.

Discussion

Our findings provide evidence for two distinct cellular targets for cGMP-induced toxicity. We show that the primary target for elevated [cGMP] in the PDE6 loss-of-function *Pde6g*$^{-/-}$ mice is the CNG channel. These observations are consistent with previous reports showing the protective effects of *Cngb1* null background on *rd1* mice (24); and are also in agreement with strategies to improve photoreceptor survival either by the shRNA knockdown of CNG channel expression in *Pde6*^{H620Q} mutant mice (25,26) or by the treatment of calcium channel blockers in *rd1* mice (42). We further demonstrated that, although there are two different isoforms of PRKG, PRKG1 constitutes most of the enzymatic activity in the retina (Fig. 4A and 4B), and that preventing *Prkg1* expression in the *Pde6g*$^{-/-}$ mice had no detectable effect in prolonging rod survival (Fig. 4C and 4D). These results are somewhat contradictory to previous studies using PRKG inhibitors on *rd1* and *rd2* mice (27). The discrepancy may be due to the presence of the minor PRKG2 isoform. However, PRKG2 transcript in the eye is low compared to that of PRKG1; further, *in situ* hybridization detected stronger PRKG2 signal in the inner nuclear and ganglion cell layers (40), suggesting that PRKG2 expression in the ONL is low. Its contribution in cGMP-induced photoreceptor cell death in *Pde6* loss-of-function mutations awaits future investigations. Together, our results suggest that excessive calcium entry through CNG channels may be the common key effector of retinal degeneration caused by *Pde6* loss-of-function mutations and perhaps other genetic mutations culminating in cGMP accumulation when the CNG channel is expressed and functional.

CNG channel loss-of-function mutations in rods and cones lead to autosomal recessive retinitis pigmentosa and achromatopsia in humans (7), respectively, wherein cell death is also preceded by elevated [cGMP]. The rate of rod cell death in *Cngb1*$^{-/-}$ appears much slower when compared to that of *Pde6* loss-of-function mutations (Fig. 2, also (35,36)), and preventing *Prkg1* expression in *Cngb1*$^{-/-}$ rods had a significant effect in prolonging rod survival and, in turn, cone survival (Figs 5 and 6). Our genetic studies provide strong support for a causal role of PRKG1 in the cGMP-induced cell death pathway in CNG channel loss-of-function mutations, whereas previous reports provided correlative evidence between PRKG1 activity and photoreceptor cell death (10,43). Why is PRKG1 involved in rod death caused by CNG channel deficiency but not *Pde6* loss-of-function when both lead to elevated [cGMP]? One possibility may be the kinetics of the different cell death pathways: the gating of CNG channel by cGMP and time-scale of Ca^{2+}-influx occurs in the timescale of milliseconds (44). This rapid action may supersede PRKG1 activation, which may require a sustained elevated [cGMP] that occurs in the *Cngb1*$^{-/-}$ but not in the rapidly dying *Pde6g*$^{-/-}$ rods.

The rescue of rods by *Prkg1* ablation in *Cngb1*$^{-/-}$ retinae was partial, indicating the involvement of other pathway(s). The nature of these pathways are not known, but may involve 1) remaining PRKG2 activity, 2) the absence of Ca^{2+} influx through the CNG channel and continuous efflux through NCKX1 creating a sustained low intracellular Ca^{2+} environment that may be detrimental (45,46), 3) Ca^{2+}-binding proteins, such as GCAPs, may be destabilized by low [Ca^{2+}] (34,47), which may lead to the overload of ubiquitination and proteasome pathway and ER stress related cell death, 4) low [Ca^{2+}]-induced constitutive cGMP synthesis by GCAPs may cause metabolic overload and mitochondrial insult (31). Identification of these additional pathways awaits future investigations.

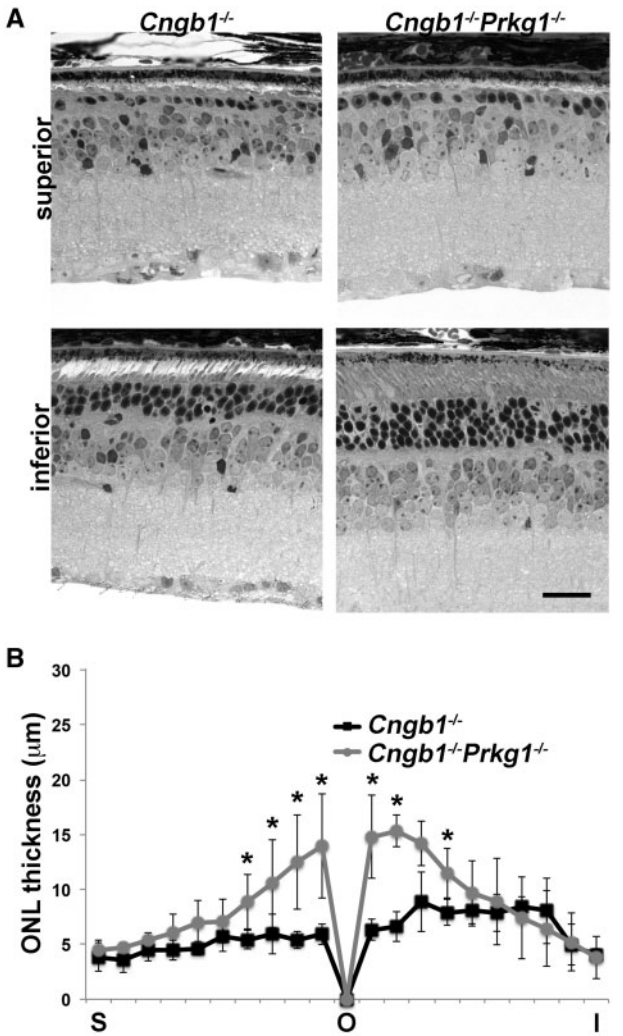

Figure 5. *Prkg1* knockout has a recuing effect on rod death in *Cngb1*$^{-/-}$ retinae. (**A**) Retinal morphology of 3 month-old age-matched *Cngb1*$^{-/-}$ and *Cngb1*$^{-/-}$*Prkg1*$^{-/-}$ littermates. Shown are images taken from the mid-superior and mid-inferior regions of the central retina. Scale bar = 20 μm. (**B**) Quantification of ONL thickness from mice of the indicated genotypes (mean ± SD, $N = 3$ for *Cngb1*$^{-/-}$ and $N = 6$ for *Cngb1*$^{-/-}$*Prkg1*$^{-/-}$. Asterisks represent $P < 0.05$, 2-tailed *t*-test. S, superior; I, inferior; O, optic nerve.

Although CNG channel is a primary target for cGMP-induced toxicity in retinae of *Pde6g*$^{-/-}$ mice, removal of CNG channel expression did not offer long-term rescue. Evidence from *Cngb1*$^{-/-}$*Prkg1*$^{-/-}$ mice illustrates a causal role of PRKG1 activity in promoting photoreceptor cell death when the channel expression is abolished. Therefore, application of CNG channel inhibitors to treat retinal degeneration caused by elevated cGMP may in turn activate PRKG and trigger cell death through this alternative pathway. Our results suggest that a combinatorial approach that utilizes both CNG channel and PRKG inhibitors may be more efficacious in the treatment of retinal degeneration caused by elevated cGMP.

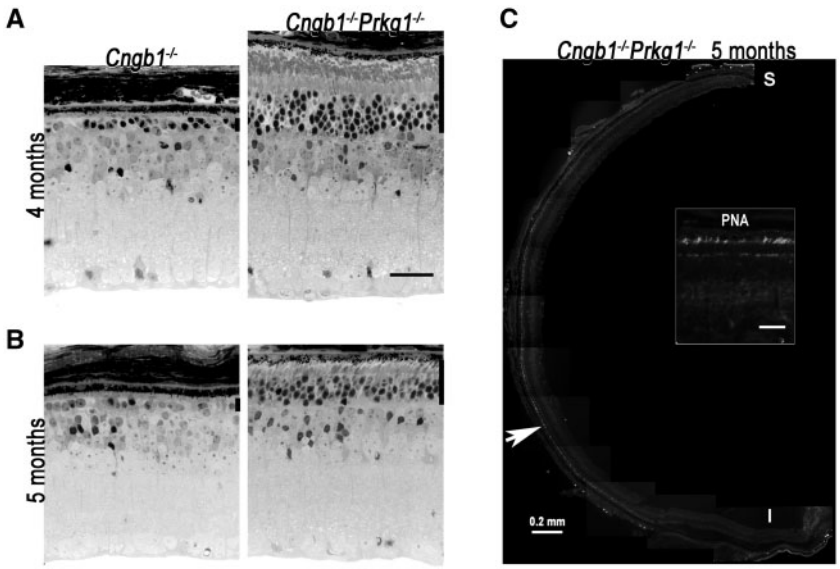

Figure 6. *Prkg1* knockout offers long-term rescue of *Cngb1*$^{-/-}$ rods. Light micrograph of retinal sections from *Cngb1*$^{-/-}$ and *Cngb1*$^{-/-}$*Prkg1*$^{-/-}$ littermates at 4- (**A**) and 5-months (**B**) of age. The remaining ONL is highlighted by the vertical bar at the right side of each panel. Scale bar = 20 μm. (**C**) Retinal section from a 5 month-old *Cngb1*$^{-/-}$*Prkg1*$^{-/-}$ mouse stained with peanut agglutinin (PNA), a cone marker. PNA staining is seen primarily in the central-inferior region of the retina (white arrow). The inset shows a higher magnification from the boxed region. S, superior; I, inferior.

In conclusion, our data show that the genetic ablation of CNG channels in *Pde6g*$^{-/-}$ mice significantly slowed retinal degeneration despite elevated cGMP levels, suggesting the uncontrolled Ca^{2+} entry through open CNG channels, rather than other signaling pathways of cGMP, is directly responsible for the early initiation of photoreceptor cell death of *Pde6g*$^{-/-}$ mice. In the absence of the CNG channels, chronically elevated cGMP levels activate *Prkg1*, leading to cell death. Our data strongly implicate two distinct cGMP-mediated cell death pathways. Identification of these cellular targets should advance therapeutic intervention strategies aimed at slowing photoreceptor cell death caused by elevated cGMP.

Materials and Methods

Animals

All experimental procedures were performed in accordance with regulations established by the National Institutes of Health. The animal protocol was approved by the University of Southern California Institutional Animal Care and Use Committee. *Pde6g*$^{-/-}$ mice were bred into the knockout background of either CNGB1 or PRKG1 genes to generate double mutant mice, termed as *Pde6g*$^{-/-}$*Cngb1*$^{-/-}$ and *Pde6g*$^{-/-}$*Prkg1*$^{-/-}$. *Cngb1* knockout mice were also bred with *Prkg1* knockout mice to generate *Cngb1*$^{-/-}$ *Prkg1*$^{-/-}$ mice.

Retinal morphology

Mice were anesthetized by isoflurane inhalation and killed by cervical dislocation, after which the superior pole of the cornea was marked by cauterization. The eyes were then enucleated, and fixed in ½ Karnovsky buffer (2.5% glutaraldehyde, 2% formaldehyde in 0.1M cacodylate buffer, pH 7.2) for 5 min. Following fixation, the cornea and lens were removed, and the remaining eyecups were further fixed overnight in ½ Karnovsky buffer at 4°C, rinsed in 0.1M cacodylate buffer, and prepared into epoxy resin blocks as described previously (48). The central retina was sectioned along the vertical meridian at 1 micron thickness and stained with Richardson stain for light microscopy. Images were acquired on an Axioplan2 microscope (Zeiss). The thickness of the outer nuclear layer (ONL) was measured based on a previously described method (49). Each hemisphere - determined by the optic nerve - was divided into ten equal segments from the optic nerve to either the superior or inferior tip, and the corresponding ONL thickness was measured for each segment. Due to the thinness of the outer nuclear layer at the optic nerve location, determination of the ten equal segments for each hemisphere excluded the first 100 μm from the optic nerve site.

cGMP ELISA

Retinae were dissected and immediately frozen in liquid N_2. Each frozen retina was homogenized in 100 μl of 6% trichloroacetic acid on ice followed by 6 times extraction with 1 ml of water-saturated ether. The aqueous extract was dried in a vacuum centrifuge (UVS 400 Universal Vacuum system). Protein levels were measured using the Pierce BCA assay (Thermo Fisher). The total cGMP amount was measured using a cyclic GMP XP Assay Kit (Cell Signaling #4360S) following manufacturer's instructions, and the value was normalized to the protein content.

PRKG activity assay

Individual retina was snap frozen in dry ice/ethanol bath and kept in −80° C. On the day of the assay, retinae were homogenized in 100 μl buffer (20 mM Tris, pH 7.4, 150 mM NaCl, 1 mM EDTA, 1 mM EGTA, 2 mM NaF, 2 mM Na_3VO_4, protease inhibitors). The supernatant was collected, and PRKG activity in 100 μg of retinal proteins was assayed using the CycLex® cGMP-dependent protein kinase assay kit following manufacturer's instructions (MBL International Corporation).

Western blots

Each isolated retina was homogenized in 150 μl buffer (150 mM NaCl, 50mM Tris pH8.0, 0.1% NP-40, 0.5% deoxycholic acid) containing 0.1 mM phenylmethane sulfonyl fluoride and complete mini protease inhibitor (Roche #11836153001). DNase I (30U, Roche) was added and incubated at room temperature for 30 min. The total protein amount of each sample was determined by the BCA™ Protein Assay Kit (Thermo Scientific #23227). An equal amount of retinal homogenate from each sample was electrophoresed on 4–12% Bis-Tris SDS-PAGE Gel (Invitrogen) followed by transfer to nitrocellulose membrane (Whatman #10402480) and incubated overnight at 4° C with the following primary antibodies: rabbit anti-PDE6 polyclonal antibody (1:1000, Cytosignal PAB-06800), rabbit anti-ROS-GC1 polyclonal antibody (1:500, Santa Cruz, sc50512), mouse Anti-$G_t\alpha$-1 antibody (1:5000, EMD4Biosciences 371740), mouse anti-CNGβ1 antibody 4B1 (1:500, a generous gift from Dr. R. Molday), rabbit anti-phospho-VASP (Ser239) antibody (1:500, Cell signaling #3114) and mouse anti-Actin antibody (1:5000, Millipore MAB1501). The membranes were then incubated with fluorescently labeled secondary antibodies (1:10,000 Li-Cor P/N926-31081) at room temperature for 1 h and detected by Odyssey infrared imaging system.

Acknowledgements

JC and SHT were supported by the National Institutes of Health.

Conflict of Interest statement. None declared.

Funding

National Institutes of Health (R01 EY12155, EY027193; R01EY018213, R01EY024698, R01EY026682 and R21AG050437), Jonas Children's Vision Care, and Bernard & Shirlee Brown Glaucoma Laboratory are supported by 5P30EY019007, 5P30CA013696, Research to Prevent Blindness (RPB) Physician-Scientist Award, unrestricted funds from RPB, New York, NY, USA. New York State [N09G-302 and N13G-275], the Foundation Fighting Blindness New York Regional Research Center Grant [C-NY05-0705-0312], the Crowley Family Fund, and the Gebroe Family Foundation.

References

1. Dizhoor, A.M., Boikov, SG, and Olshevskaya, E.V. (1998) Constitutive activation of photoreceptor guanylate cyclase by Y99C mutant of GCAP-1. Possible role in causing human autosomal dominant cone degeneration. *J. Biol. Chem.*, **273**, 17311–17314.
2. Olshevskaya, E.V., Calvert, PD, Woodruff, M.L., Peshenko, I.V., Savchenko, A.B., Makino, C.L., Ho, Y.S., Fain, G.L. and Dizhoor, A.M. (2004) The Y99C mutation in guanylyl cyclase-activating protein 1 increases intracellular Ca2+ and causes photoreceptor degeneration in transgenic mice. *J. Neurosci.*, **24**, 6078–6085.
3. Sokal, I., Dupps, WJ, Grassi, M.A., Brown, J., Jr, Affatigato, L.M., Roychowdhury, N., Yang, L., Filipek, S., Palczewski, K., Stone, E.M. and Baehr, W. (2005) A novel GCAP1 missense mutation (L151F) in a large family with autosomal dominant cone-rod dystrophy (adCORD). *Invest. Ophthalmol. Vis. Sci.*, **46**, 1124–1132.
4. Sokal, I., Li, N., Surgucheva, I., Warren, M.J., Payne, A.M., Bhattacharya, S.S., Baehr, W. and Palczewski, K. (1998) GCAP1 (Y99C) mutant is constitutively active in autosomal dominant cone dystrophy. *Mol. Cell*, **2**, 129–133.
5. McLaughlin, M.E., Ehrhart, T.L., Berson, E.L. and Dryja, T.P. (1995) Mutation spectrum of the gene encoding the beta subunit of rod phosphodiesterase among patients with autosomal recessive retinitis pigmentosa. *Proc. Natl Acad. Sci. U S A*, **92**, 3249–3253.
6. Huang, S.H., Pittler, S.J., Huang, X., Oliveira, L., Berson, E.L. and Dryja, T.P. (1995) Autosomal recessive retinitis pigmentosa caused by mutations in the alpha subunit of rod cGMP phosphodiesterase. *Nat. Genet.*, **11**, 468–471.
7. Biel, M. and Michalakis, S. (2007) Function and dysfunction of CNG channels: insights from channelopathies and mouse models. *Mol. Neurobiol.*, **35**, 266–277.
8. Doonan, F., Donovan, M. and Cotter, T.G. (2005) Activation of multiple pathways during photoreceptor apoptosis in the rd mouse. *Invest. Ophthalmol. Vis. Sci.*, **46**, 3530–3538.
9. Woodruff, M.L., Olshevskaya, E.V., Savchenko, A.B., Peshenko, I.V., Barrett, R., Bush, R.A., Sieving, P.A., Fain, G.L. and Dizhoor, A.M. (2007) Constitutive excitation by Gly90Asp rhodopsin rescues rods from degeneration caused by elevated production of cGMP in the dark. *J Neurosci.*, **27**, 8805–8815.
10. Xu, J., Morris, L., Thapa, A., Ma, H., Michalakis, S., Biel, M., Baehr, W., Peshenko, I.V., Dizhoor, A.M. and Ding, X.Q. (2013) cGMP accumulation causes photoreceptor degeneration in CNG channel deficiency: evidence of cGMP cytotoxicity independently of enhanced CNG channel function. *J. Neurosci.*, **33**, 14939–14948.
11. Pugh, E.N., Jr. and Lamb, T.D. (1990) Cyclic GMP and calcium: the internal messengers of excitation and adaptation in vertebrate photoreceptors. *Vision Res.*, **30**, 1923–1948.
12. Yau, K.W. and Baylor, D.A. (1989) Cyclic GMP-activated conductance of retinal photoreceptor cells. *Ann. Rev. Neurosci.*, **12**, 289–327.
13. Yau, K.W. and Nakatani, K. (1984) Cation selectivity of light-sensitive conductance in retinal rods. *Nature*, **309**, 352–354.
14. Schnetkamp, P.P. (2004) The SLC24 Na+/Ca2+-K+ exchanger family: vision and beyond. *Pflugers Archiv.*, **447**, 683–688.
15. Vinberg, F., Wang, T., Molday, R.S., Chen, J. and Kefalov, V.J. (2015) A new mouse model for stationary night blindness with mutant Slc24a1 explains the pathophysiology of the associated human disease. *Hum. Mol. Genet.*, **24**, 5915–5929.
16. Dizhoor, A.M., Olshevskaya, E.V., Henzel, W.J., Wong, S.C., Stults, J.T., Ankoudinova, I. and Hurley, J.B. (1995) Cloning, sequencing, and expression of a 24-kDa Ca(2+)-binding protein activating photoreceptor guanylyl cyclase. *J. Biol. Chem.*, **270**, 25200–25206.
17. Gorczyca, W.A., Gray-Keller, M.P., Detwiler, P.B. and Palczewski, K. (1994) Purification and physiological evaluation of a guanylate cyclase activating protein from retinal rods. *Proc. Natl Acad. Sci. U S A.*, **91**, 4014–4018.
18. Palczewski, K., Subbaraya, I., Gorczyca, W.A., Helekar, B.S., Ruiz, C.C., Ohguro, H., Huang, J., Zhao, X., Crabb, J.W., Johnson, R.S. *et al.* (1994) Molecular cloning and characterization of retinal photoreceptor guanylyl cyclase-activating protein. *Neuron*, **13**, 395–404.
19. Mendez, A., Burns, M.E., Sokal, I., Dizhoor, A.M., Baehr, W., Palczewski, K., Baylor, D.A. and Chen, J. (2001) Role of guanylate cyclase-activating proteins (GCAPs) in setting the flash sensitivity of rod photoreceptors. *Proc. Natl Acad. Sci. U S A.*, **98**, 9948–9953.

20. Burns, M.E., Mendez, A., Chen, J. and Baylor, D.A. (2002) Dynamics of cyclic GMP synthesis in retinal rods. *Neuron*, **36**, 81–91.
21. Haynes, L.W., Kay, A.R. and Yau, K.W. (1986) Single cyclic GMP-activated channel activity in excised patches of rod outer segment membrane. *Nature*, **321**, 66–70.
22. Zimmerman, A.L. and Baylor, D.A. (1986) Cyclic GMP-sensitive conductance of retinal rods consists of aqueous pores. *Nature*, **321**, 70–72.
23. Warren, R. and Molday, R.S. (2002) Regulation of the rod photoreceptor cyclic nucleotide-gated channel. *Adv. Exp. Med. Biol.*, **514**, 205–223.
24. Paquet-Durand, F., Beck, S., Michalakis, S., Goldmann, T., Huber, G., Muhlfriedel, R., Trifunovic, D., Fischer, M.D., Fahl, E., Duetsch, G. *et al.* (2011) A key role for cyclic nucleotide gated (CNG) channels in cGMP-related retinitis pigmentosa. *Hum. Mol. Genet.*, **20**, 941–947.
25. Tosi, J., Davis, R.J., Wang, N.K., Naumann, M., Lin, C.S. and Tsang, S.H. (2011) shRNA knockdown of guanylate cyclase 2e or cyclic nucleotide gated channel alpha 1 increases photoreceptor survival in a cGMP phosphodiesterase mouse model of retinitis pigmentosa. *J. Cell. Mol. Med.*, **15**, 1778–1787.
26. Tosi, J., Sancho-Pelluz, J., Davis, R.J., Hsu, C.W., Wolpert, K.V., Sengillo, J.D., Lin, C.S. and Tsang, S.H. (2011) Lentivirus-mediated expression of cDNA and shRNA slows degeneration in retinitis pigmentosa. *Exp. Biol. Med. (Maywood)*, **236**, 1211–1217.
27. Paquet-Durand, F., Hauck, S.M., van Veen, T., Ueffing, M. and Ekstrom, P. (2009) PKG activity causes photoreceptor cell death in two retinitis pigmentosa models. *J. Neurochem.*, **108**, 796–810.
28. Farber, D.B. (1995) From mice to men: the cyclic GMP phosphodiesterase gene in vision and disease. The Proctor Lecture. *Invest. Ophthalmol. Vis. Sci.*, **36**, 263–275.
29. Farber, D.B. and Lolley, R.N. (1974) Cyclic guanosine monophosphate: elevation in degenerating photoreceptor cells of the C3H mouse retina. *Science*, **186**, 449–451.
30. Koch, S., Sothilingam, V., Garcia Garrido, M., Tanimoto, N., Becirovic, E., Koch, F., Seide, C., Beck, S.C., Seeliger, M.W., Biel, M. *et al.* (2012) Gene therapy restores vision and delays degeneration in the CNGB1(-/-) mouse model of retinitis pigmentosa. *Hum. Mol. Genet.*, **21**, 4486–4496.
31. Thapa, A., Morris, L., Xu, J., Ma, H., Michalakis, S., Biel, M. and Ding, X.Q. (2012) Endoplasmic reticulum stress-associated cone photoreceptor degeneration in cyclic nucleotide-gated channel deficiency. *J. Biol. Chemi.*, **287**, 18018–18029.
32. Arango-Gonzalez, B., Trifunovic, D., Sahaboglu, A., Kranz, K., Michalakis, S., Farinelli, P., Koch, S., Koch, F., Cottet, S., Janssen-Bienhold, U. *et al.* (2014) Identification of a common non-apoptotic cell death mechanism in hereditary retinal degeneration. *PloS One*, **9**, e112142.
33. Tsang, S.H., Gouras, P., Yamashita, C.K., Kjeldbye, H., Fisher, J., Farber, D.B. and Goff, S.P. (1996) Retinal degeneration in mice lacking the gamma subunit of the rod cGMP phosphodiesterase. *Science*, **272**, 1026–1029.
34. Wang, T. and Chen, J. (2014) Induction of the unfolded protein response by constitutive G-protein signaling in rod photoreceptor cells. *J. Biol. Chem.*, **289**, 29310–29321.
35. Huttl, S., Michalakis, S., Seeliger, M., Luo, D.G., Acar, N., Geiger, H., Hudl, K., Mader, R., Haverkamp, S., Moser, M. *et al.* (2005) Impaired channel targeting and retinal degeneration in mice lacking the cyclic nucleotide-gated channel subunit CNGB1. *J. Neurosci.*, **25**, 130–138.
36. Zhang, Y., Molday, L.L., Molday, R.S., Sarfare, S.S., Woodruff, M.L., Fain, G.L., Kraft, T.W. and Pittler, S.J. (2009) Knockout of GARPs and the beta-subunit of the rod cGMP-gated channel disrupts disk morphogenesis and rod outer segment structural integrity. *J. Cell Sci.*, **122**, 1192–1200.
37. Pfeifer, A., Klatt, P., Massberg, S., Ny, L., Sausbier, M., Hirneiss, C., Wang, G.X., Korth, M., Aszodi, A., Andersson, K.E. *et al.* (1998) Defective smooth muscle regulation in cGMP kinase I-deficient mice. *EMBO J.*, **17**, 3045–3051.
38. Carter-Dawson, L.D. and LaVail, M.M. (1979) Rods and cones in the mouse retina. I. Structural analysis using light and electron microscopy. *J. Comp. Neurol.*, **188**, 245–262.
39. Hofmann, F., Feil, R., Kleppisch, T. and Schlossmann, J. (2006) Function of cGMP-dependent protein kinases as revealed by gene deletion. *Physiol. Rev.*, **86**, 1–23.
40. Gamm, D.M., Barthel, L.K., Raymond, P.A. and Uhler, M.D. (2000) Localization of cGMP-dependent protein kinase isoforms in mouse eye. *Invest. Ophthalmol. Vis. Sci.*, **41**, 2766–2773.
41. Smolenski, A., Bachmann, C., Reinhard, K., Honig-Liedl, P., Jarchau, T., Hoschuetzky, H. and Walter, U. (1998) Analysis and regulation of vasodilator-stimulated phosphoprotein serine 239 phosphorylation in vitro and in intact cells using a phosphospecific monoclonal antibody. *J. Biol. Chem.*, **273**, 20029–20035.
42. Frasson, M., Sahel, J.A., Fabre, M., Simonutti, M., Dreyfus, H. and Picaud, S. (1999) Retinitis pigmentosa: rod photoreceptor rescue by a calcium-channel blocker in the rd mouse. *Nat. Med.*, **5**, 1183–1187.
43. Ma, H., Butler, M.R., Thapa, A., Belcher, J., Yang, F., Baehr, W., Biel, M., Michalakis, S. and Ding, X.Q. (2015) cGMP/protein kinase G signaling suppresses inositol 1,4,5-trisphosphate receptor phosphorylation and promotes endoplasmic reticulum stress in photoreceptors of cyclic nucleotide-gated channel-deficient mice. *J. Biol. Chem.*, **290**, 20880–20892.
44. Karpen, J.W., Zimmerman, A.L., Stryer, L. and Baylor, D.A. (1988) Gating kinetics of the cyclic-GMP-activated channel of retinal rods: flash photolysis and voltage-jump studies. *Proc. Natl Acad. Sci. U S A.*, **85**, 1287–1291.
45. Lisman, J. and Fain, G. (1995) Support for the equivalent light hypothesis for RP. *Nat Med*, **1**, 1254–1255.
46. Woodruff, M.L., Wang, Z., Chung, H.Y., Redmond, T.M., Fain, G.L. and Lem, J. (2003) Spontaneous activity of opsin apoprotein is a cause of Leber congenital amaurosis. *Nat. Genet.*, **35**, 158–164.
47. Hoyo, N.L., Lopez-Begines, S., Rosa, J.L., Chen, J. and Mendez, A. (2014) Functional EF-hands in neuronal calcium sensor GCAP2 determine its phosphorylation state and subcellular distribution in vivo, and are essential for photoreceptor cell integrity. *PLoS Genet.*, **10**, e1004480.
48. Concepcion, F., Mendez, A. and Chen, J. (2002) The carboxyl-terminal domain is essential for rhodopsin transport in rod photoreceptors. *Vis. Res.*, **42**, 417–426.
49. Chen, J., Shi, G., Concepcion, F.A., Xie, G. and Oprian, D. (2006) Stable rhodopsin/arrestin complex leads to retinal degeneration in a transgenic mouse model of autosomal dominant retinitis pigmentosa. *J. Neurosci.*, **26**, 11929–11937.